Measurement of $B(D_s^+ \to \mu^+ \nu_\mu)$

L. Widhalm,[10] I. Adachi,[7] H. Aihara,[42] T. Aushev,[17,12] A. M. Bakich,[38] V. Balagura,[12] E. Barberio,[20] A. Bay,[17] I. Bedny,[1] V. Bhardwaj,[32] U. Bitenc,[13] S. Blyth,[24] A. Bozek,[26] M. Bračko,[19,13] J. Brodzicka,[7] T. E. Browder,[6] Y. Chao,[25] A. Chen,[23] W. T. Chen,[23] B. G. Cheon,[5] R. Chistov,[12] I.-S. Cho,[47] Y. Choi,[37] J. Dalseno,[20] M. Dash,[46] A. Drutskoy,[3] S. Eidelman,[1] P. Goldenzweig,[3] B. Golob,[18,13] H. Ha,[15] J. Haba,[7] K. Hayasaka,[21] H. Hayashii,[22] M. Hazumi,[7] D. Heffernan,[31] Y. Hoshi,[40] W.-S. Hou,[25] Y. B. Hsiung,[25] H. J. Hyun,[16] T. Iijima,[21] K. Inami,[21] A. Ishikawa,[34] H. Ishino,[43] R. Itoh,[7] M. Iwasaki,[42] Y. Iwasaki,[7] D. H. Kah,[16] J. H. Kang,[47] P. Kapusta,[26] N. Katayama,[7] H. Kawai,[2] T. Kawasaki,[28] H. Kichimi,[7] S. K. Kim,[36] Y. J. Kim,[4] K. Kinoshita,[3] S. Korpar,[19,13] P. Križan,[18,13] P. Krokovny,[7] R. Kumar,[32] C. C. Kuo,[23] Y. Kuroki,[31] A. Kuzmin,[1] Y.-J. Kwon,[47] J. Lee,[36] J. S. Lee,[37] M. J. Lee,[36] S. E. Lee,[36] T. Lesiak,[26] S.-W. Lin,[25] C. Liu,[35] D. Liventsev,[12] F. Mandl,[10] A. Matyja,[26] S. McOnie,[38] W. Mitaroff,[10] H. Miyake,[31] H. Miyata,[28] Y. Miyazaki,[21] R. Mizuk,[12] G. R. Moloney,[20] E. Nakano,[30] M. Nakao,[7] Z. Natkaniec,[26] S. Nishida,[7] O. Nitoh,[45] S. Noguchi,[22] S. Ogawa,[39] T. Ohshima,[21] S. Okuno,[14] H. Ozaki,[7] P. Pakhlov,[12] G. Pakhlova,[12] H. Palka,[26] C. W. Park,[37] H. Park,[16] K. S. Park,[37] L. S. Peak,[38] R. Pestotnik,[13] L. E. Piilonen,[46] H. Sahoo,[6] Y. Sakai,[7] O. Schneider,[17] R. Seidl,[8,33] A. Sekiya,[22] K. Senyo,[21] M. Shapkin,[11] H. Shibuya,[39] J.-G. Shiu,[25] J. B. Singh,[32] A. Somov,[3] S. Stanič,[29] M. Starič,[13] T. Sumiyoshi,[44] S. Y. Suzuki,[7] F. Takasaki,[7] N. Tamura,[28] M. Tanaka,[7] G. N. Taylor,[20] Y. Teramoto,[30] I. Tikhomirov,[12] K. Trabelsi,[7] S. Uehara,[7] T. Uglov,[12] Y. Unno,[5] S. Uno,[7] P. Urquijo,[20] Y. Usov,[1] G. Varner,[6] K. Vervink,[17] C. H. Wang,[24] M.-Z. Wang,[25] P. Wang,[9] Y. Watanabe,[14] R. Wedd,[20] E. Won,[15] B. D. Yabsley,[38] H. Yamamoto,[41] Y. Yamashita,[27] Z. P. Zhang,[35] V. Zhilich,[1] A. Zupanc,[13] and O. Zyukova[1]

(The Belle Collaboration)

[1]*Budker Institute of Nuclear Physics, Novosibirsk*
[2]*Chiba University, Chiba*
[3]*University of Cincinnati, Cincinnati, Ohio 45221*
[4]*The Graduate University for Advanced Studies, Hayama*
[5]*Hanyang University, Seoul*
[6]*University of Hawaii, Honolulu, Hawaii 96822*
[7]*High Energy Accelerator Research Organization (KEK), Tsukuba*
[8]*University of Illinois at Urbana-Champaign, Urbana, Illinois 61801*
[9]*Institute of High Energy Physics, Chinese Academy of Sciences, Beijing*
[10]*Institute of High Energy Physics, Vienna*
[11]*Institute of High Energy Physics, Protvino*
[12]*Institute for Theoretical and Experimental Physics, Moscow*
[13]*J. Stefan Institute, Ljubljana*
[14]*Kanagawa University, Yokohama*
[15]*Korea University, Seoul*
[16]*Kyungpook National University, Taegu*
[17]*École Polytechnique Fédérale de Lausanne (EPFL), Lausanne*
[18]*Faculty of Mathematics and Physics, University of Ljubljana, Ljubljana*
[19]*University of Maribor, Maribor*
[20]*University of Melbourne, School of Physics, Victoria 3010*
[21]*Nagoya University, Nagoya*
[22]*Nara Women's University, Nara*
[23]*National Central University, Chung-li*
[24]*National United University, Miao Li*
[25]*Department of Physics, National Taiwan University, Taipei*
[26]*H. Niewodniczanski Institute of Nuclear Physics, Krakow*
[27]*Nippon Dental University, Niigata*
[28]*Niigata University, Niigata*
[29]*University of Nova Gorica, Nova Gorica*
[30]*Osaka City University, Osaka*
[31]*Osaka University, Osaka*
[32]*Panjab University, Chandigarh*
[33]*RIKEN BNL Research Center, Upton, New York 11973*
[34]*Saga University, Saga*
[35]*University of Science and Technology of China, Hefei*

[36]Seoul National University, Seoul
[37]Sungkyunkwan University, Suwon
[38]University of Sydney, Sydney, New South Wales
[39]Toho University, Funabashi
[40]Tohoku Gakuin University, Tagajo
[41]Tohoku University, Sendai
[42]Department of Physics, University of Tokyo, Tokyo
[43]Tokyo Institute of Technology, Tokyo
[44]Tokyo Metropolitan University, Tokyo
[45]Tokyo University of Agriculture and Technology, Tokyo
[46]Virginia Polytechnic Institute and State University, Blacksburg, Virginia 24061
[47]Yonsei University, Seoul

(Received 20 February 2008; published 17 June 2008)

We present a measurement of the branching fraction $\mathcal{B}(D_s^+ \to \mu^+ \nu_\mu)$ using a 548 fb^{-1} data sample collected by the Belle experiment at the KEKB e^+e^- collider. The D_s momentum is determined by reconstruction of the system recoiling against $DK\gamma X$ in events of the type $e^+e^- \to D_s^* DKX$, $D_s^* \to D_s\gamma$, where X represents additional pions or photons from fragmentation. This full-reconstruction method provides high resolution in the neutrino momentum and thus good background separation, equivalent to that achieved by experiments at the tau-charm factories. We obtain the branching fraction $\mathcal{B}(D_s^+ \to \mu^+ \nu_\mu) = [6.44 \pm 0.76(\text{stat}) \pm 0.57(\text{syst})] \times 10^{-3}$, implying a D_s decay constant of $f_{D_s} = [275 \pm 16(\text{stat}) \pm 12(\text{syst})]$ MeV.

DOI: 10.1103/PhysRevLett.100.241801 PACS numbers: 13.20.Fc

One of the important goals of particle physics is the precise measurement and understanding of the Cabibbo-Kobayashi-Maskawa (CKM) matrix elements, fundamental parameters of the Standard Model (SM). To interpret precise experimental results on decays of B mesons in terms of the CKM matrix elements, theoretical calculations of form factors, and decay constants (usually based on lattice gauge theory—LQCD, see, e.g., [1]) are needed. Decays of charmed hadrons in turn enable tests of the predictions for analogous quantities in the charm sector.

The purely leptonic decay $D_s^+ \to \ell^+ \nu_\ell$ (the charge-conjugate mode is implied throughout this Letter) is theoretically rather clean; in the SM, the decay is mediated by a single virtual $W^\pm$ boson. The decay rate is given by

$$\Gamma(D_s^+ \to \ell^+ \nu_\ell) = \frac{G_F^2}{8\pi} f_{D_s}^2 m_\ell^2 m_{D_s} \left(1 - \frac{m_\ell^2}{m_{D_s}^2}\right)^2 |V_{cs}|^2, \quad (1)$$

where G_F is the Fermi coupling constant, m_ℓ and m_{D_s} are the masses of the lepton and of the D_s meson, respectively. V_{cs} is the corresponding CKM matrix element, while all effects of the strong interaction are accounted for by the decay constant f_{D_s}. While the decay rate is tiny for electrons due to the strong helicity suppression, and since the detection of τ's involves additional neutrinos, the muon mode is experimentally the cleanest and the most accessible. Decays with electrons can be used to study the backgrounds.

Recently, an LQCD calculation of f_{D_s} with a significantly improved precision was performed [2]. Its accuracy exceeds that of individual experimental results by at least a factor of 3. Measurements of charmed meson decay rates with an accuracy that matches the precision of theoretical calculations are thus necessary to check and further test theoretical methods.

The analysis described in this Letter uses data from the Belle experiment [3] at the KEKB collider [4] corresponding to 548 fb^{-1}. Similar analyses have also been performed by the CLEO-c [5] and *BABAR* [6] experiments. We study the decay $D_s^+ \to \mu^+ \nu_\mu$ using the full-reconstruction recoil method first established in the study of semileptonic D mesons [7]. The method of fully-reconstructed events has lower efficiency than methods using partial reconstruction [6]. However, this method allows a measurement of the branching fraction without the need for normalization to another decay mode, and thus avoids additional, difficult to estimate systematic uncertainties. Furthermore, a high signal-to-background ratio, comparable to the measurements performed at the $D_s^+ D_s^{*-}$ production threshold [5], can be achieved, which compensates for the loss of statistics.

The Belle detector is a large-solid-angle magnetic spectrometer that consists of a silicon vertex detector (SVD), a 50-layer central drift chamber (CDC), an array of aerogel threshold Cherenkov counters (ACC), a barrel-like arrangement of time-of-flight scintillation counters (TOF), and an electromagnetic calorimeter comprised of CsI(Tl) crystals (ECL) located inside a superconducting solenoid coil that provides a 1.5 T magnetic field. An iron flux-return located outside of the coil is instrumented to detect K_L^0 mesons and to identify muons (KLM). The detector is described in detail elsewhere [3]. Two inner detector configurations were used. A 2.0 cm diameter beam pipe and a 3-layer silicon vertex detector were used for the first sample of 156 fb^{-1}, while a 1.5 cm beam pipe, a 4-layer silicon detector, and a small-cell inner drift chamber were used to record the remaining 392 fb^{-1} [8].

This analysis uses events of the type $e^+e^- \to D_s^* D^{\pm,0} K^{\pm,0} X$, where X can be any number of additional pions from fragmentation, and up to one photon [9]. The *tag side* consists of a D and a K meson (in any charge combination) while the *signal side* is a D_s^* meson decaying to $D_s\gamma$. Reconstructing the tag side and allowing any possible set of particles in X, the signal side is identified by reconstruction of the recoil mass, using the known beam momentum and four-momentum conservation.

Tracks are detected with the CDC and the SVD. They are required to have at least one associated hit in the SVD and an impact parameter with respect to the interaction point of less than 2 cm in the radial direction and less than 4 cm in the beam direction. Tracks are also required to have momenta in the laboratory frame greater than 100 MeV/c. A likelihood ratio for a given track to be a kaon or pion, $\mathcal{L}(K, \pi)$, is obtained by combining specific ionization energy loss measurements in the CDC, light yield measurements from the ACC, and time-of-flight information from the TOF [10]. We require $\mathcal{L}(K, \pi) > 0.5$ for kaon candidates. The momentum of the lepton candidates is required to be larger than 500 MeV/c. For electron identification, we use position, cluster energy, shower shape in the ECL, combined with track momentum and dE/dx measurements in the CDC and hits in the ACC. For muon identification, we extrapolate the CDC track to the KLM and compare the measured range and transverse deviation in the KLM with the expected values. Photons are required to have energies in the laboratory frame of at least 50–150 MeV, depending on the polar angle region in the ECL. Neutral pion candidates are reconstructed using photon pairs with invariant mass within ± 10 MeV/c^2 of the nominal π^0 mass. Neutral kaon candidates are reconstructed using charged pion pairs with invariant mass within ± 30 MeV/c^2 of the nominal K^0 mass.

Charged and neutral tag-side D mesons are reconstructed in $D \to Kn\pi$ decays with $n = 1, 2, 3$ (total branching fraction $\approx 25\%$). Mass windows were optimized for each channel separately, and a mass-constrained vertex fit (requiring a confidence level greater than 0.1%) is applied to the D meson to improve the momentum resolution. D_s^*-candidates are not directly reconstructed: we construct the mass of the system recoiling against DKX, using the known beam momentum, and require a value within ± 150 MeV/c^2 of the nominal D_s^* mass [11]. A recoil mass $M_{\rm rec}(Y)$ is defined as the magnitude of the four-momentum $p_{\rm beams} - p_Y$, for an arbitrary set of reconstructed particles Y. Here, $p_{\rm beams}$ is the momentum of the initial e^+e^- system. Since at this point in the reconstruction X can be any set of remaining pions and photons, there are usually a large number of combinatorial possibilities. These are reduced by requiring the presence of a photon that is consistent with the decay $D_s^* \to D_s\gamma$, where the D_s mass lies within ± 150 MeV/c^2 of its nominal value [11]. Further selection criteria are applied on the momenta of particles in the e^+e^- rest frame; for the primary K meson, the momentum should be smaller than 2 GeV/c, for the D meson larger than 2 GeV/c and for the D_s meson larger than 3 GeV/c. The energy of the photon from $D_s^* \to D_s\gamma$ in the lab frame is required to be larger than 150 MeV, irrespective of its polar angle. To further improve the recoil momentum resolution, inverse [12] mass-constrained vertex fits are then performed for the D_s^* and D_s, requiring a confidence level greater than 1%. After applying these selection criteria, the average number of combinatorial reconstruction possibilities is approximately 2 per event. The sample is further divided into a right- (RS) and wrong-sign (WS) part. If the primary K meson is charged, both it and the D meson are required to have flavor (strangeness or charm, respectively) opposite to the D_s^*, in order to be counted in the right-sign sample; all other combinations are wrong-sign. If the primary K meson is a K_S^0, the assignment is based on the relative flavors of the D and D_s^* mesons alone. The flavor of the D_s^* is fixed by the total charge of X, assuming overall charge conservation for the event.

Within this sample of tagged inclusive D_s decays (called D_s-tags in what follows), decays of the type $D_s \to \mu\nu_\mu$ are selected by requiring another charged track that is identified as a muon and has the same charge as the D_s candidate. No additional charged particles are allowed in the event. Remaining photons not used in the reconstruction described above are allowed only if their total energy is smaller than $1.0/m$ GeV, where m is the number of such particles. After these selections, in almost all cases only one combinatorial reconstruction possibility remains. Figure 1 shows the mass spectra of $M_{\rm rec}(DKX\gamma)$ (corresponding to the candidate D_s mass) and of $M_{\rm rec}(DKX\gamma\mu)$ (corresponding to the neutrino candidate mass).

We define n_X as the number of *primary* particles in the event, where primary means that the particle is not a daughter of any particle reconstructed in the event. The minimal value for n_X is three corresponding to a $e^+e^- \to D_s^* DK$ event without any further particles from fragmentation. The upper limit for n_X is determined by the reconstruction efficiency; Monte Carlo (MC) simulation shows that the number of reconstructed signal events is negligible for $n_X > 10$. As the efficiency is very sensitive to n_X, it is crucial to use MC simulation that correctly reflects the n_X distribution observed in the data. Unfortunately, the details of fragmentation processes are not very well understood, and standard MC events show substantial differences in their n_X distributions compared to the data. Furthermore, the true (generated) n_X^T value differs from the reconstructed n_X^R, as particles can be lost or incorrectly assigned. Thus, the measured (reconstructed) n_X^R distribution has to be deconvoluted so that the analysis can be done in bins of n_X^T to avoid bias in the results.

To extract the number of D_s-tags as a function of n_X^T in data, two-dimensional simulated distributions in n_X^R (rang-

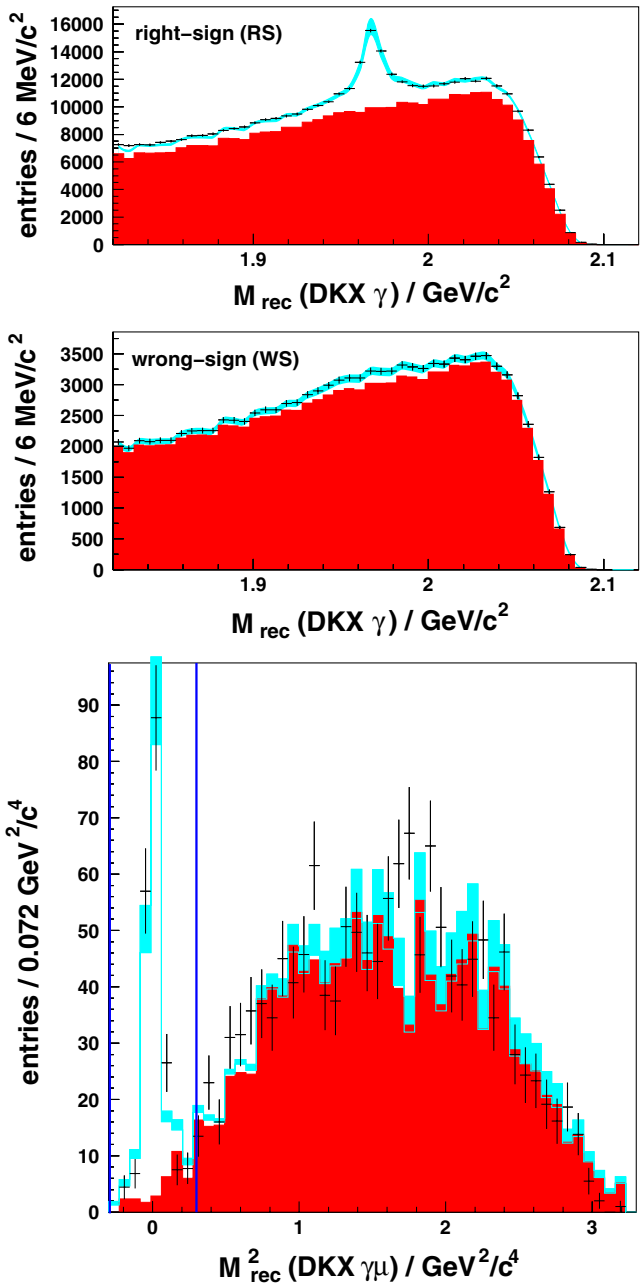

FIG. 1 (color online). Top: recoil mass spectrum for D_s-tags (for both RS and WS samples). Bottom: spectrum of missing mass squared for $D_s^+ \to \mu^+\nu_\mu$ candidates for the selected data. Error bars represent the statistical errors. The dark-shaded areas show the fitted background; the light-shaded bands show the fit to signal and background with systematic uncertainties. The vertical lines indicate the signal regions.

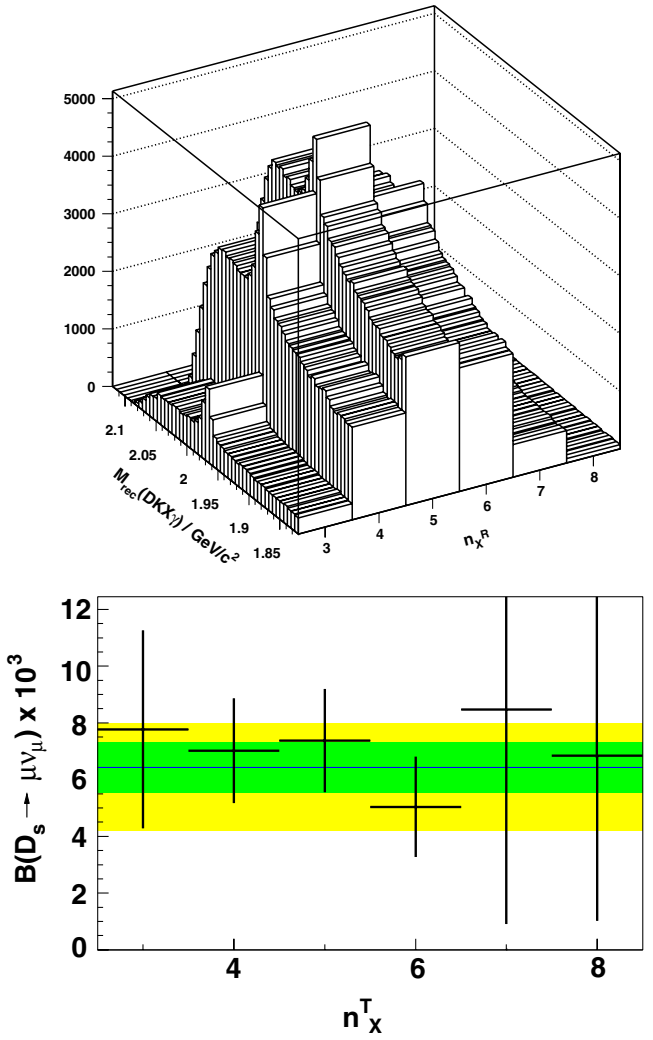

FIG. 2 (color online). Top: two-dimensional distribution in the recoil mass and n_X^R for selected D_s-tags. Bottom: $\mathcal{B}(D_s \to \mu\nu_\mu)$ as a function of n_X^T; the final result is shown as the dark-shaded region. For comparison, the 2006 world average value [11] and its error are shown as the light-shaded region in the background.

ing from 3 to 8) and the recoil mass $M_{\rm rec}(DKX\gamma)$ are fitted to the RS and WS data distributions. The two-dimensional data distribution of D_s-tags is shown in Fig. 2, top. Signal shapes for different values of n_X^T (ranging from 3 to 9 [13]) are modeled with generic MC simulation [14], which has been filtered at the generator level for events of the type $e^+e^- \to D_s^* DKX$. The weights of these components, $w_i^{D_s}$, $i = 3, \ldots, 8$, are free parameters in the fit to the data. As a model for the background in the RS sample, the WS data sample is used. The relative normalizations of WS and RS (which vary with n_X^R) are another six fit parameters. Since the WS sample contains some signal (≈10% of the RS signal), these signal components for different n_X^T values are also included in the fit as independent parameters. As a cross check, the fit has also been performed using generic MC RS-sample backgrounds, which gives a negligible change in the results. A further cross check involved the random division of the MC sample into two halves, using the shapes of the first half to fit the signal in the second. The resulting weights as a function of n_X^T fit to a constant of 0.990 ± 0.046, which agrees well with the expectation of 1. The total number of reconstructed D_s-tags in data is calculated as

$$N_{D_s}^{\mathrm{rec}} = \sum_{i=3}^{8} w_i^{D_s} N_{D_s}^{\mathrm{MC},i}, \tag{2}$$

where $N_{D_s}^{\mathrm{MC},i}$ represents the total number of reconstructed filtered MC events that were generated with $n_X^T = i$ (regardless of the reconstructed n_X^R), and $w_i^{D_s}$ is the fitted weight of this component.

To fit the number of $D_s \to \mu\nu_\mu$ events as a function of n_X^T, two-dimensional histograms in n_X^R and the recoil mass $M_{\mathrm{rec}}(DKX\gamma\mu)$ are used. The shape of the signal is modeled with a distribution from the signal MC simulation. As MC studies show, the background under the $\mu\nu_\mu$ signal peak consists primarily of non-D_s decays ($\approx$18% of signal), leptonic τ decays (where the τ decays to a muon and two neutrinos, $\approx$7%), and semileptonic D_s decays (where the additional hadrons have low momenta and remain undetected, $\approx$3.6%). Hadronic D_s decays (with one hadron misidentified as a muon) are a rather small background component ($\leq$2% of signal). Except for hadronic decays, which are negligible, all backgrounds are common to the $e\nu_e$ mode, which is suppressed by a factor of $\mathcal{O}(10^5)$. Thus, the $e\nu_e$ sample provides a good model of the $\mu\nu_\mu$ background that has to be corrected only for kinematical and efficiency differences. Including this corrected shape in the fit, the total number of fitted $\mu\nu_\mu$ events in data is given by

$$N_{\mu\nu}^{\mathrm{rec}} = \sum_{i=3}^{8} w_i^{\mu\nu} N_{\mu\nu}^{\mathrm{MC},i}, \tag{3}$$

where $N_{\mu\nu}^{\mathrm{MC},i}$ represents the total number of reconstructed signal MC events that were generated in the i-th bin of n_X^T (regardless of the reconstructed n_X^R) and $w_i^{\mu\nu}$ is the fitted weight of this component. The fitted values of $w_i^{\mu\nu}$ deviate up to 3.4 standard deviations from the mean value, reflecting the limited accuracy of the description of fragmentation in MC simulation.

The numerical result for $N_{D_s}^{\mathrm{rec}}$ is $32100 \pm 870(\mathrm{stat}) \pm 1210(\mathrm{syst})$, that for $N_{\mu\nu}^{\mathrm{rec}}$ is $169 \pm 16(\mathrm{stat}) \pm 8(\mathrm{syst})$. The statistical errors reflect the small number of data signal candidates. The systematic errors are due to the limited statistics of WS data, MC signal, and background samples. The errors were estimated by varying the bin contents of data and MC distributions and repeating the fits. This procedure takes into account the non-negligible correlations between the fitted weights.

As the branching fraction of $D_s \to \mu\nu_\mu$ used for the generation of MC events is known, the branching fraction in data can be determined using the following formula:

$$\mathcal{B}(D_s \to \mu\nu_\mu) = \frac{N_{\mu\nu}^{\mathrm{rec}}}{\bar{\epsilon}_{\mu\nu} N_{D_s}^{\mathrm{rec}}} = \frac{N_{\mu\nu}^{\mathrm{rec}}}{N_{\mu\nu}^{\mathrm{MC,rec}}} \mathcal{B}_{\mathrm{MC}}(D_s \to \mu\nu_\mu), \tag{4}$$

where $\mathcal{B}_{\mathrm{MC}}(D_s \to \mu\nu_\mu) = 0.51\%$ and $N_{\mu\nu}^{\mathrm{MC,rec}}$ is the number of reconstructed $\mu\nu_\mu$ events in MC simulation, weighted according to the fit to data, i.e.,

$$N_{\mu\nu}^{\mathrm{MC,rec}} = \sum_{i=3}^{8} w_i^{D_s} N_{\mu\nu}^{\mathrm{MC},i}. \tag{5}$$

The average efficiency for the reconstruction of $D_s \to \mu\nu_\mu$ decays, $\bar{\epsilon}_{\mu\nu}$, is not needed explicitly for the computation of the branching fraction [15]. The final result is

$$\mathcal{B}(D_s \to \mu\nu_\mu) \times 10^3 = 6.44 \pm 0.76(\mathrm{stat}) \pm 0.57(\mathrm{syst}). \tag{6}$$

The quoted statistical error reflects the statistical uncertainty of the fitted weights $w_i^{D_s}$ and $w_i^{\mu\nu}$, including their correlations. The systematic error combines the contributions due to the statistical uncertainties of data and MC background samples (0.29), the statistical uncertainty of the signal MC distribution (0.41), muon tracking and identification efficiency (0.18), and possible differences in relative rates of individual D_s decay modes between MC simulation and data, as well as small differences between the simulated and observed shapes of the $M_{\mathrm{rec}}(DKX\gamma)$ distribution (0.19). Since the branching fraction is determined relative to the number of D_s-tags, the systematic uncertainties in the reconstruction of the tag side cancel. Differences in the neutrino peak resolution between data and simulation have been found to have a negligible effect on the systematic error.

Figure 2 (bottom) shows the branching fraction determined in bins of n_X^T. The result is stable within the errors; note that the errors shown for the n_X^T bins are correlated. As a cross check, the branching fraction in a limited range $n_X^T \leq 6$ has also been determined as $[6.54 \pm 0.76(\mathrm{stat}) \pm 0.57(\mathrm{syst})] \times 10^{-3}$, which agrees well with the result given above.

In conclusion, we have studied events of the type $e^+e^- \to D_s^* D^{\pm,0} K^{\pm,0} X$, $D_s^* \to D_s\gamma$ with $X = n\pi(\gamma)$ where the D_s is identified in the recoil of the remainder of the event. Normalizing to this sample of D_s-tags, the branching fraction of $D_s \to \mu\nu_\mu$ is measured to be $[6.44 \pm 0.76(\mathrm{stat}) \pm 0.57(\mathrm{syst})] \times 10^{-3}$, which is in good agreement with the world average value of $(6.1 \pm 1.9) \times 10^{-3}$ [11] and also compatible with recent results from *BABAR* $(6.74 \pm 1.09) \times 10^{-3}$ [7] and CLEO-c $(5.94 \pm 0.73) \times 10^{-3}$ [6]. Finally, we obtain the decay constant f_{D_s}, using Eq. (1) (with $|V_{cs}| = 0.9730$ [11])

$$f_{D_s} = [275 \pm 16(\mathrm{stat}) \pm 12(\mathrm{syst})]\ \mathrm{MeV}. \tag{7}$$

A simple average of the decay constants following from the cited individual measurements is $f_{D_s} = (276 \pm 11)$ MeV. The measurements are performed under different experimental conditions or using different methods, justifying the assumption of uncorrelated systematic uncertainties. Recent unquenched LQCD calculation [2] results in $f_{D_s} = (241 \pm 3)$ MeV. This value is lower than the experimental world average. More precise measurements

are needed to establish a discrepancy, which will become possible in the near future at both B and tau-charm factories. If the discrepancy persists, LQCD calculations should be reexamined. Alternatively, if the LQCD calculations are found to be sound, the possibility of contributions from new particles, which increase the $D_s \to \mu\nu_\mu$ rate, may need to be considered [16].

We thank the KEKB group for excellent operation of the accelerator, the KEK cryogenics group for efficient solenoid operations, and the KEK computer group and the NII for valuable computing and Super-SINET network support. We acknowledge support from MEXT and JSPS (Japan); ARC and DEST (Australia); NSFC and KIP of CAS (Contract Nos. 10575109 and IHEP-U-503, China); DST (India); the BK21 program of MOEHRD, and the CHEP SRC and BR (Grant No. R01-2005-000-10089-0) programs of KOSEF (Korea); KBN (Contract No. 2P03B 01324, Poland); MES and RFAAE (Russia); ARRS (Slovenia); SNSF (Switzerland); NSC and MOE (Taiwan); and DOE (USA).

[1] A. S. Kronfeld (Fermilab Lattice Collaboration), J. Phys. Conf. Ser. **46**, 147 (2006).
[2] E. Follana *et al.* (HPQCD and UKQCD Collaboration), Phys. Rev. Lett. **100**, 062002 (2008).
[3] A. Abashian *et al.* (Belle Collaboration), Nucl. Instrum. Methods Phys. Res., Sect. A **479**, 117 (2002).
[4] S. Kurokawa and E. Kikutani (Belle Collaboration), Nucl. Instrum. Methods Phys. Res., Sect. A **499**, 1 (2003), and other papers in this volume.
[5] M. Artuso *et al.* (CLEO-c Collaboration), Phys. Rev. Lett. **99**, 071802 (2007).
[6] B. Aubert *et al.* (BABAR Collaboration), Phys. Rev. Lett. **98**, 141801 (2007).
[7] L. Widhalm *et al.* (Belle Collaboration), Phys. Rev. Lett. **97**, 061804 (2006).
[8] Z. Natkaniec *et al.* (Belle SVD2 Group), Nucl. Instrum. Methods Phys. Res., Sect. A **560**, 1 (2006).
[9] It has been found that events with additional kaons or more than one photon have a poor signal/background ratio and have been therefore excluded.
[10] E. Nakano, Nucl. Instrum. Methods Phys. Res., Sect. A **494**, 402 (2002).
[11] W.-M. Yao *et al.* (Particle Data Group), J. Phys. G **33**, 1 (2006).
[12] The fit is called inverse since it uses information from the mother and sister particles, rather than information about daughter particles as is usually the case.
[13] The upper limit of 9 is chosen because the bin $n_X^T = 9$ has some overlap with $n_X^R \leq 8$. The corresponding fitted weight turns out to be negligible and is neglected in further analysis.
[14] R. Brun *et al.*, GEANT 3.21, CERN Report No. DD/EE/84-1, 1984.
[15] As defined in Eq. (4), the average efficiency $\bar{\epsilon}_{\mu\nu} = \sum_{i=1}^{8}(w_i^{D_s} N_{\mu\nu}^{\mathrm{MC},i}) / \sum_{i=1}^{8}(w_i^{D_s} N_{\mu\nu}^{\mathrm{MC},i}/\epsilon_i)$.
[16] B. A. Dobrescu and A. S. Kronfeld, arXiv:0803.0512 [Phys. Rev. Lett. (to be published)].